



## Research Article

## Nasal delivery of broadly neutralizing antibodies protects mice from lethal challenge with SARS-CoV-2 delta and omicron variants



Jia Lu<sup>a,1</sup>, Qiangling Yin<sup>b,1</sup>, Rongjuan Pei<sup>c,d,1</sup>, Qiu Zhang<sup>a</sup>, Yuanyuan Qu<sup>e</sup>, Yongbing Pan<sup>a</sup>, Lina Sun<sup>b</sup>, Ding Gao<sup>c</sup>, Cuiqin Liang<sup>c</sup>, Jingwen Yang<sup>c</sup>, Wei Wu<sup>b</sup>, Jiandong Li<sup>b</sup>, Zongqiang Cui<sup>c</sup>, Zejun Wang<sup>a</sup>, Xinguo Li<sup>a</sup>, Dexin Li<sup>b,d</sup>, Shiwen Wang<sup>b,d</sup>, Kai Duan<sup>a</sup>, Wuxiang Guan<sup>c,d,\*</sup>, Mifang Liang<sup>b,d,\*</sup>, Xiaoming Yang<sup>a,\*</sup>

<sup>a</sup> National Engineering Technology Research Center for Combined Vaccines, Wuhan Institute of Biological Products Co. Ltd., Wuhan, 430070, China

<sup>b</sup> State Key Laboratory for Molecular Virology and Genetic Engineering, National Institute for Viral Disease Control and Prevention, Chinese Center for Disease Control and Prevention, Beijing, 102206, China

<sup>c</sup> Center for Emerging Infectious Diseases, Wuhan Institute of Virology, Chinese Academy of Sciences, Wuhan, 430071, China

<sup>d</sup> CDC-WIV Joint Research Center for Emerging Diseases and Biosafety, Wuhan, 430071, China

<sup>e</sup> Institution of Infectious Diseases, Shenzhen Bay Laboratory, Shenzhen, 518107, China

## ARTICLE INFO

## Keywords:

Coronavirus disease 2019 (COVID-2019)  
Severe acute respiratory syndrome coronavirus 2 (SARS-CoV-2)  
Prophylactic protection  
Omicron variant  
K18-hACE2

## ABSTRACT

Multiple new variants of severe acute respiratory syndrome coronavirus 2 (SARS-CoV-2) have constantly emerged, as the delta and omicron variants, which have developed resistance to currently gained neutralizing antibodies. This highlights a critical need to discover new therapeutic agents to overcome the variants mutations. Despite the availability of vaccines against coronavirus disease 2019 (COVID-19), the use of broadly neutralizing antibodies has been considered as an alternative way for the prevention or treatment of SARS-CoV-2 variants infection. Here, we show that the nasal delivery of two previously characterized broadly neutralizing antibodies (F61 and H121) protected K18-hACE2 mice against lethal challenge with SARS-CoV-2 variants. The broadly protective efficacy of the F61 or F61/F121 cocktail antibodies was evaluated by lethal challenge with the wild strain (WIV04) and multiple variants, including beta (B.1.351), delta (B.1.617.2), and omicron (B.1.1.529) at 200 or 1000 TCID<sub>50</sub>, and the minimum antibody administration doses (5–1.25 mg/kg body weight) were also evaluated with delta and omicron challenge. Fully prophylactic protections were found in all challenged groups with both F61 and F61/H121 combination at the administration dose of 20 mg/kg body weight, and corresponding mice lung viral RNA showed negative, with almost all alveolar septa and cavities remaining normal. Furthermore, low-dose antibody treatment induced significant prophylactic protection against lethal challenge with delta and omicron variants, whereas the F61/H121 combination showed excellent results against omicron infection. Our findings indicated the potential use of broadly neutralizing monoclonal antibodies as prophylactic and therapeutic agent for protection of current emerged SARS-CoV-2 variants infection.

## 1. Introduction

Coronavirus disease 2019 (COVID-19), an acute viral disease caused by severe acute respiratory syndrome coronavirus 2 (SARS-CoV-2), has emerged worldwide as an unprecedented public health emergency, with over 404 million confirmed cases and 5.78 million deaths (WHO, 2022). The rapid international transmission and emergence of SARS-CoV-2 variants poses a serious challenge to global health and may render our

current antibody and vaccine strategies ineffective (Andreato et al., 2021; Piccoli et al., 2020; Weisblum et al., 2020; Starr et al., 2021). As of January 10, 2022, multiple new variants of concern (VOCs) associated with enhanced transmissibility and increased virulence have emerged, such as the alpha (B.1.1.7), beta (B.1.351), gamma (P.1), delta (B.1.617.2), and omicron variants (B.1.1.529) (WHO, 2022). All five of these VOCs harbor mutations in the receptor binding domain (RBD) and the N-terminal domain, which serve as the dominant neutralization

\* Corresponding authors.

E-mail addresses: [guanwx@wh.iov.cn](mailto:guanwx@wh.iov.cn) (W. Guan), [liangmf@ivdc.chinacdc.cn](mailto:liangmf@ivdc.chinacdc.cn) (M. Liang), [yangxiaoming@sinopharm.com](mailto:yangxiaoming@sinopharm.com) (X. Yang).

<sup>1</sup> Jia Lu, Qiangling Yin, Rongjuan Pei contributed equally to this work.

target and facilitate antibody production in response to antisera or vaccines (He et al., 2004; Du et al., 2007; Jiang et al., 2012; Wang et al., 2020). Among these variants, omicron was quickly recognized as a VOC owing to the presence of more than 30 changes in the spike protein of the virus (Callaway, 2021) as well as the sharp rise in the number of cases observed in South Africa (Viana et al., 2022). Initial modeling suggests that the omicron variant exhibits a 13-fold increase in viral infectivity and is 2.8 times more infectious than the delta variant (Chen et al., 2021). The prevalence of the omicron variant has increased to 80%, making this variant the predominant strain worldwide (GISAIID, 2022). The spike mutation K417 N (also detected in the beta variant) and the mutation E484A are predicted to have overwhelmingly disruptive effects, making omicron more likely to exhibit vaccine breakthrough (Chen et al., 2021). Moreover, this variant has been reported to be at increased risk of transmission and to reduce neutralization by monoclonal antibody therapy, convalescent sera, and post-vaccination sera (Hoffmann et al., 2021; Planas et al., 2021). Hence, there is an urgent need for antiviral interventions, such as broadly neutralizing monoclonal antibodies, to prevent and treat COVID-19.

In recent years, monoclonal antibodies targeting viral surface proteins have been proven to be effective in blocking the invasion of viruses when used as prophylactic drugs (Ku et al., 2021; Kwon, 2021). Indeed, a nasal spray preparation of an antibody against influenza virus was shown to directly establish a defense in the respiratory tract and lungs, thereby preventing viral infection (Leyva-Grado et al., 2015). In addition, local administration significantly reduced the drug administered dose and promoted the drug-use safety (Tiwari et al., 2012). Similar to influenza viruses, SARS-CoV-2 is also a respiratory virus. Nasal spray preventive drugs may have applications in management of the COVID-19 pandemic. However, only seven monoclonal antibody combinations have currently been approved or authorized for emergency use worldwide, and most of these preparations are intravenous drugs to be administered for COVID-19 treatment and postexposure prevention (Drozdal et al., 2021; NIH, 2021).

Previously, we described two broadly neutralizing antibodies, F61 and H121, which showed high neutralizing capacity along with a favorable biochemical profile for large-scale production and clinical use (Qu et al., 2021). Therefore, in this study, to estimate the *in vivo* preventive effects of F61 and H121, we tested intranasal administration of these antibodies in K18-hACE2 mice. Our results showed that intranasal administration of F61 and H121 provided potent *in vivo* protection and broader coverage over currently circulating VOCs, including the omicron strain. These results highlight F61 and H121 as potential preventive antibodies with broad neutralizing activity.

## 2. Materials and methods

### 2.1. Cells and viruses

Human embryonic kidney 293 (HEK293) cells and Vero E6 cells were initially purchased from the American Type Culture Collection (ATCC, Manassas, VA, USA). HEK293 cells were cultured at 37 °C in an atmosphere containing 5% CO<sub>2</sub> with Dulbecco's modified Eagle's medium (DMEM; Life Technologies, USA) supplemented with 10% heat inactivated fetal bovine serum (FBS; Life Technologies) and 1% penicillin/streptomycin (Life Technologies) or in EXPI293 expression medium (Life Technologies). Cells were passaged every two days. The wild strain (WIV04) and three SARS-CoV-2 variants of interest, including the beta (B.1.351), delta (B.1.617.2), and omicron variants (B.1.1.529), were used for viral challenge in animal experiments. All viruses were isolated from nasopharyngeal and oropharyngeal samples from patients with COVID-19 and deposited by Wuhan Institute of Biological Products Co. Ltd. or Wuhan Institute of Virology. SARS-CoV-2 was propagated in Vero E6 cells and was harvested 3–5 days postinfection. Virus-induced cytopathic effect was observed under a reverse-phase light microscope. Virus titers were determined by median tissue culture infectious dose 50

(TCID<sub>50</sub>) tests with Vero E6 cells. Briefly, the virus was grown in Vero E6 cells and maintained in DMEM (Sigma-Aldrich, St. Louis, MO, USA) containing 10% FBS (Sigma-Aldrich), 1% antibiotic-antimycotic (Sigma-Aldrich), and 1% L-glutamine (Sigma-Aldrich). Cells were cultured at 37 °C in an atmosphere containing 5% CO<sub>2</sub> for 96 h. Virus stocks were titrated using TCID<sub>50</sub> assays, as previously described (Lei et al., 2021) and were found to be 10<sup>6.58</sup>–10<sup>7.33</sup> TCID<sub>50</sub>/mL.

### 2.2. Human antibodies

F61 and H121 monoclonal antibodies were screened from peripheral blood mononuclear cells isolated from convalescent patients with COVID-19 using the phage display technique, as previously described (Qu et al., 2021). F61 and H121 bound to different epitopes. Specifically, F61 recognized a linear epitope that overlapped the angiotensin converting enzyme 2 (ACE2)-binding sites on the RBD. Both the light and heavy chains of F61 participated in binding to RBD. H121 recognized a conformational epitope located distant from the ACE2 binding region and mainly recognized by the heavy chain. Both F61 and H121 exhibited high affinity and broadly neutralizing capacity. The cocktail of F61 and H121 (at a ratio of 1:1) exhibited synergistic neutralization. F61 and H121 exhibited efficient neutralizing activity against the delta variant and slightly decreased (although not significantly altered) neutralizing activity against B.1.351 (at a ratio of more than 0.25). Synergistic use of F61 and H121 exhibited similar neutralizing activities against the B.1.1.7, B.1.351, and wild virus. Recombinant monoclonal antibodies were produced in HEK293 cells (ATCC) by transfecting pairs of the IgG1 heavy and light chain expression plasmids. Human antibodies purified by Protein-G (GE Healthcare, USA) affinity chromatography were stored at –80 °C until use.

### 2.3. Mice

C57BL/6 N (B6) and heterozygous transgenic B6 mice expressing human ACE2 (hACE2) via the cytokeratin 18 promoter (K18) (K18-hACE2) (Hassan et al., 2020; Sun et al., 2020) were purchased from GemPharmatech Co., Ltd. Company. Male K18-hACE2 mice (6–8 weeks old) were used for mouse protection experiments, and male C57BL/6 N mice (6–8 weeks old) were used for *in vivo* bioavailability assays and for analysis of the distribution of administered monoclonal antibodies.

### 2.4. *In vivo* bioavailability and distribution of administered monoclonal antibodies

The F61 antibody was conjugated with Alexa Fluor 70 dye for *in vivo* imaging studies. Briefly, 1.78 mg/mL solution of F61 in phosphate-buffered saline (PBS; pH 7.4) was reacted with Alexa Fluor 750 succinimidyl ester (AF750-NHS; Thermo Fisher Scientific) in the presence of 3% dimethyl sulfoxide and 10% sodium bicarbonate buffer (v/v, pH 8.3) at a molar ratio of 1:10 (protein to fluorescent probe) at room temperature for 1 h. Unreacted dye was removed by dialysis, and the labeled antibody was washed in PBS and concentrated with an Amicon ultra centrifugal filter unit (molecular weight cut off: 10 kDa). All procedures were performed under dimmed light. C57BL/6 N mice (6–8 weeks old, male; GemPharmatech Co., Ltd. Company) were anesthetized by inhalation of 2% isoflurane and placed in a supine position. The mice were administered Alexa Fluor 750-labeled F61 into both nostrils using a fine pipet tip (50 µL total) to achieve a final antibody dose of 1.25, 5, or 10 mg/kg body weight. The mice were then imaged at 2 min, 16 min, 2 h, 24 h, 48 h, 72 h, and 96 h after administration (fluorescence excitation wavelength = 740 nm, emission wavelength = 790 nm, auto-exposure setting, n = 4 mice/group) using an IVIS Lumina XRMS Imager (PerkinElmer). At the time of euthanasia, the heart, lungs, liver, spleen, kidneys, brain, jejunum, urocyt, and nasal cavities were excised and imaged. Regions of interest (ROIs) were drawn, and the average radiant efficiency [(p/s/cm<sup>2</sup>/sr)/(µW/cm<sup>2</sup>)] was measured. This parameter

represents the sum of the radiance from each pixel inside the ROI divided by the number of pixels. All images were processed using Living Image software (PerkinElmer), and the same fluorescence threshold was applied for group comparison.

### 2.5. Protection against SARS-CoV-2 lethal challenge in mice

Mouse protection experiments were approved by the Experimental Animal Welfare and Ethical Review Board of Wuhan Institute of Biological Products Co. Ltd. (protocol no. WIBP-AII442021005). Animals were humanely euthanized according to the guidelines established by the Chinese Veterinary Medical Association. Studies were performed in an animal biosafety level 3 containment facility at Wuhan Institute of Biological Products Co. Ltd.

To evaluate the prophylactic effects of monoclonal antibodies, four different SARS-CoV-2 strains (wild, beta, delta, and omicron strains) were used in challenge experiments. Male K18-hACE2 mice (6–8 weeks old) were randomly distributed into groups ( $n = 3–6$  mice/group). At 2 h after administration of monoclonal antibodies, mice were anesthetized with isofurane and then administered 50  $\mu$ L SARS-CoV-2 in two challenge doses (200 or  $10^3$  TCID<sub>50</sub>/mouse) via intranasal route. For challenge with the wild strain and beta variant, 50  $\mu$ L of either 20 mg/kg F61 or 20 mg/kg F61+H121 (ratio of 1:1) or vehicle (PBS) was administered to each mouse via intranasal route at 2 h before challenge. For challenge with the delta variant, 50  $\mu$ L of the antibodies at different concentrations (1.25, 5, 10, or 20 mg/kg F61 or F61+H121) was administered to each mouse via intranasal route at 2 h before challenge. For challenge with the omicron variant, 50  $\mu$ L of the antibodies at different concentrations (5 and 20 mg/kg F61 or F61+H121) was administered to each mouse via intranasal route at 2 h before challenge.

Mice were monitored every day for body weight changes and clinical signs of disease until all the mice in the control group died. Mice that lost greater than or equal to 25% of their initial body weight were humanely euthanized. At the end point of the experiment, all remaining animals in the monoclonal antibody-administered group received an overdose of isofurane and were humanely euthanized. Lungs and brains were collected from each mouse postmortem. Tissues were stored at  $-80^\circ\text{C}$  until further analysis.

### 2.6. Tissue sample preparation

Tissue homogenates were generated using the Tissue Lyzer II (Qiagen, Gaithersburg, MD, USA). Briefly, 1000  $\mu$ L PBS was added to each sample (lungs, 0.01–0.04 g) along with Tungsten carbide 3 mm beads (Qiagen). Samples were homogenized at a speed of 10 Hz for 10 min and then centrifuged at  $15,000\times g$  for 10 min. Supernatants were collected, aliquoted, and stored at  $-80^\circ\text{C}$  until further analysis.

### 2.7. RNA extraction and quantitative reverse transcription polymerase chain reaction (qRT-PCR)

Total RNA was extracted from tissues homogenates of lungs using an RNA/DNA Purification Kit (Magnetic Bead) (cat no. DA0623; Daan Gene Co., Ltd., China), and qRT-PCR was performed using a Detection Kit for 2019-nCoV (PCR-Fluorescence) (Fast) (cat no. DA0992; Daan Gene Co., Ltd.) following the manufacturer's instructions. Samples were processed in duplicate using the following cycling protocol:  $50^\circ\text{C}$  for 2 min,  $95^\circ\text{C}$  for 2 min, followed by 42 cycles at  $95^\circ\text{C}$  for 5 s and  $60^\circ\text{C}$  for 10 s. Viral RNA concentrations (copies/mL) in the lungs of mice were determined using RNA standards for SARS-CoV-2 (Bdsbiotech Co. Ltd., Guangzhou, China). The qRT-PCR results were read according to the Daan Kit criteria, the negative results in this manuscript description mean no signal detected (0 copy) or the CT values of both *N* and *ORF1ab* genes were over 38, corresponding viral RNA copies were under the limitation of the detection (LOD,  $10^{2.7}$  copies/mL).

### 2.8. Pathological examination

Autopsies were performed in an animal biosafety level 3 laboratory. Lungs were placed in 10% buffered formalin solution and fixed for at least 72 h, and paraffin sections (3–4  $\mu$ m in thickness) were prepared routinely. Hematoxylin and eosin staining was used to identify histopathological changes in the lungs. The histopathology of the lung tissue was observed by light microscopy.

### 2.9. Statistical analysis

All statistical analysis was performed using GraphPad Prism 8. All statistical tests are described in the relevant figure legends.

## 3. Results

### 3.1. Biodistribution tracking of monoclonal antibody F61 in mice

To determine the Bio-distribution of antibodies in mice after intranasal administration, different doses of Alexa Fluor® 750 labeled F61 was delivered and the levels of fluorescently labeled antibody were determined at different time points after antibody administration. Whole-body images showed that 2 min after intranasal administration, the monoclonal antibodies were mainly distributed in the nasal passages for the three monoclonal antibody administration groups. In the 5 and 10 mg/kg group, the monoclonal antibodies began to enter the lungs at 16 min after administration (Fig. 1A). At 24 h after administration, the monoclonal antibodies were mainly distributed in the lungs (Fig. 1B, E, H). Notably, *ex vivo* images showed that labeled monoclonal antibodies were still detected in the lungs at 48 h after administration in the 1.25 mg/kg group (Fig. 1D, G, J).

We then further assessed the dynamic distributions of antibodies in mice after intranasal administration of the lowest dose of monoclonal antibody. The fluorescence signals in mice after administration was imaged and quantified. In the 2 h group, the antibody was mainly distributed in the lungs [ $209.52 \times 10^8 \pm 122.93 \times 10^8$  (p/s/cm<sup>2</sup>/sr)/( $\mu\text{W}/\text{cm}^2$ )], followed by the liver ( $9.46 \times 10^8 \pm 2.62 \times 10^8$ ) and nasal cavity ( $8.71 \times 10^8 \pm 6.34 \times 10^8$ ; Fig. 1K, O). In the 24 h group, the antibody levels in the lungs, liver, and nasal cavities decreased (40.78%, 29.30%, and 81.51% respectively), and the antibody was detected in the urocyt ( $5.22 \times 10^8 \pm 2.83 \times 10^8$ ; Fig. 1L, P). In the 48 h group, the antibody levels in the lungs, liver, and nasal cavities showed persistent decreases (76.05%, 61.22%, and 91.90% respectively; Fig. 1M, Q). In the 96 h group, monoclonal antibodies were still detected in the lungs ( $23.46 \times 10^8 \pm 13.55 \times 10^8$ ) and liver ( $3.51 \times 10^8 \pm 0.69 \times 10^8$ ) and were barely detectable in other organs (Fig. 1N, R).

### 3.2. In vivo characterization of F61 and F61/H121 antibodies protection efficacy against wild strain and beta variant

To evaluate the protection efficacy of the human monoclonal antibodies F61 and F61/H121 combinations *in vivo*, the K18-hACE2 mice was selected as the animal model for this study, in which human ACE2 expression is driven by the cytokeratin 18 gene promoter (Hassan et al., 2020; Sun et al., 2020). We first gave K18-hACE2 mice a single high dose of antibodies via intranasal route as a prophylactic model, then challenged them with 200 or 1000 TCID<sub>50</sub> of SARS-CoV-2 WIV04 strain or beta variant, and monitored the body weight and survival percent till all mice in control group died. We found that when giving the mice a high dose of F61 or F61/H121 (20 mg/kg body weight), all mice survived, regardless of the dose (200 or 1000 TCID<sub>50</sub>) for mice inoculated with the wild strain (WIV04; Fig. 2A, C) or the beta variant (B.1.351; Fig. 2E, G); none of the mice in the PBS group survived (Fig. 2A, C, E, G). We also found that all antibody groups protected K18-hACE2 mice against body weight loss caused by WIV04 (Fig. 2B, D) and B.1.351 (Fig. 2F, H). The body weights of mice in the PBS group were significantly reduced

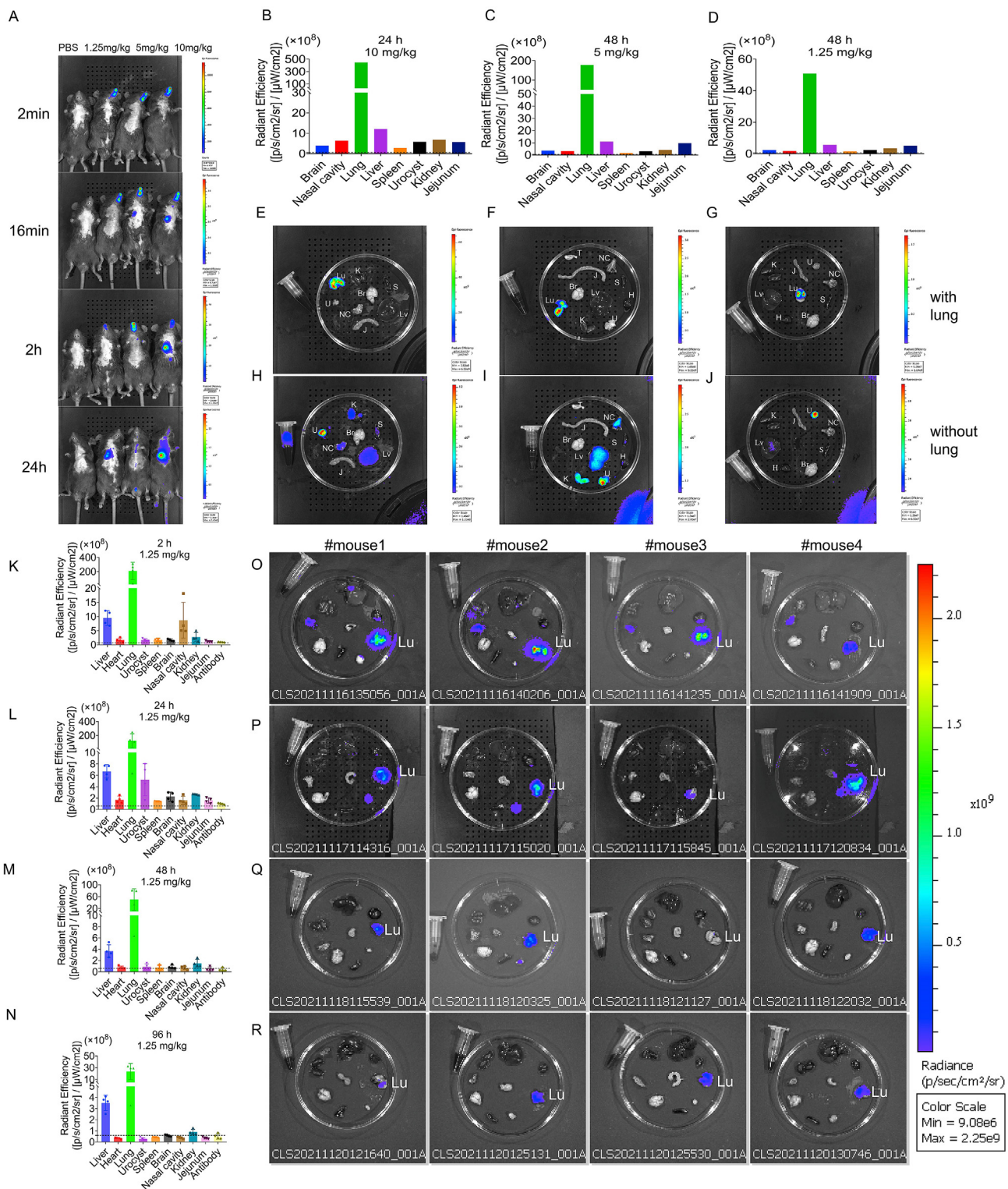


**Fig. 1.** Evaluation of the biodistribution of F61 monoclonal antibodies in mice. **A** Representative whole-body images. **B–D** Quantification of fluorescence signals in mice after intranasal delivery of different doses and at different time points (**B**: 24 h, 10 mg/kg; **C**: 48 h, 5 mg/kg; **D**: 48 h, 1.25 mg/kg). **E–J** Representative *ex vivo* images. 24 h, 10 mg/kg (**E, H**); 48 h, 5 mg/kg (**I, F**); 48 h, 1.25 mg/kg (**G, J**). **K–N** Quantification of the average radiant efficiency of different organs at different time points (**K**: 2 h, **L**: 24 h, **M**: 48 h, **N**: 96 h) after nasal delivery of F61 (1.25 mg/kg). **O–R** *Ex vivo* imaging of different organs at different time points (**O**: 2 h, **P**: 24 h, **Q**: 48 h, **R**: 96 h) after nasal delivery of F61 (1.25 mg/kg). Br, brain; H, heart; K, kidney; Lu, lung; Lv, liver; NC, nasal cavity; S, spleen; J, jejunum; U, urocyt. Data are means  $\pm$  standard deviations in four mice, as determined by Student's *t*-test. Dashed line: average autofluorescence of organs.

beginning on day 4, and body weights continued to decrease until death. The body weights of mice in the monoclonal antibody administration groups were significantly different from those in the PBS control group

on days 4 and 5 post infection ( $P < 0.05$ ; Fig. 2B, D, F, H). Note that we concluded that the death of two mice receiving 1000 TCID<sub>50</sub> WIV04 challenge (Fig. 2C, F61) was not related to the virus (two mice fought, cut

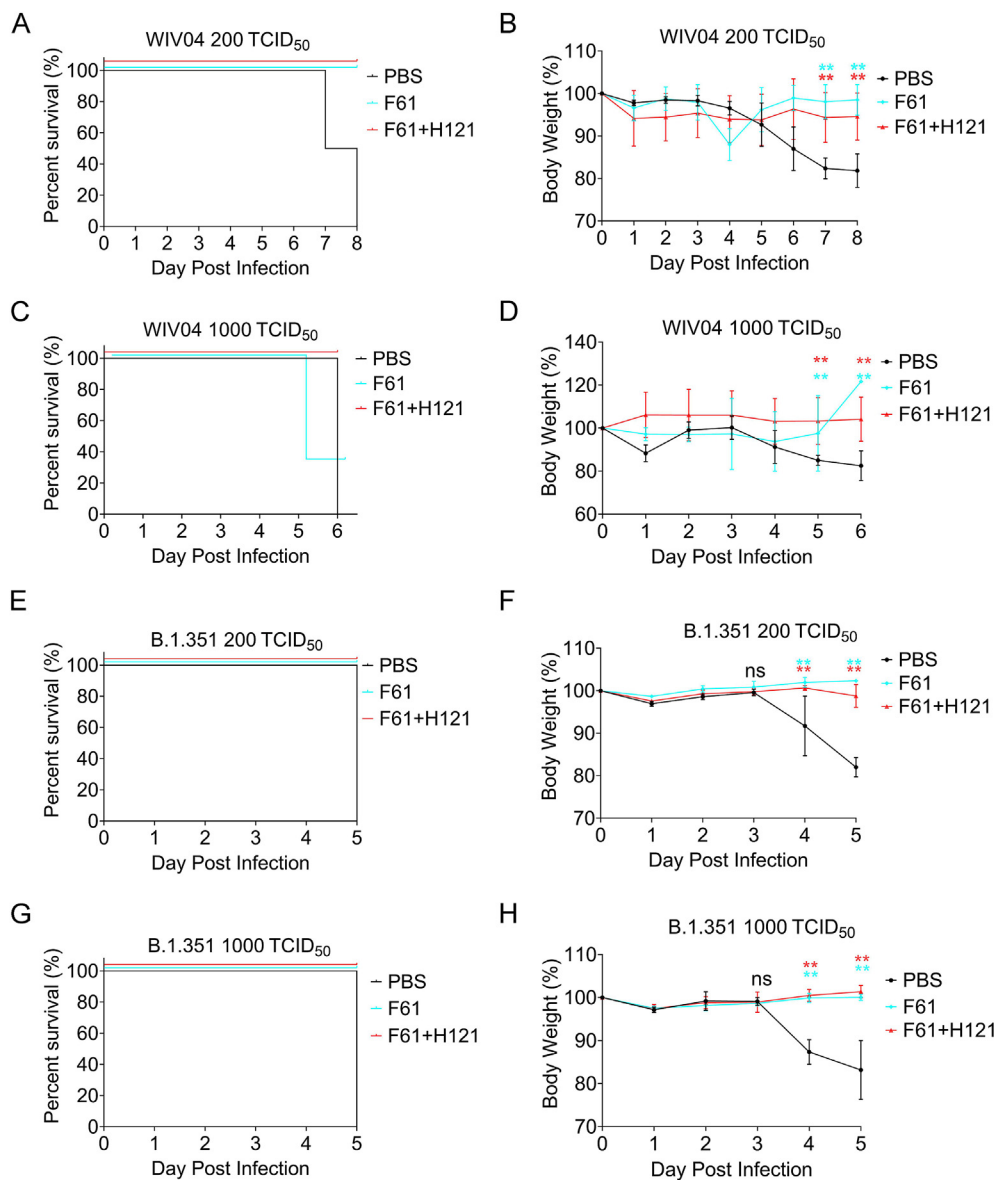


**Fig. 2.** Body weights and survival in mice treated with F61 or F61+H121 monoclonal antibodies in a prophylactic analysis of challenge with the wild strain (WIV04) or beta variant (B.1.351). **A–D** Body weights and survival curves of K18-hACE2 mice treated with 20 mg/kg F61 or F61+H121 via intranasal route before infection with 200 TCID<sub>50</sub> (**A, B**) or 1000 TCID<sub>50</sub> (**C, D**) of the wild strain of SARS-CoV-2 (WIV04). **E–H**, Body weights and survival curves of K18-hACE2 mice treated with 20 mg/kg F61 or F61+H121 via intranasal route before infection with 200 TCID<sub>50</sub> (**E, F**) or 1000 TCID<sub>50</sub> (**G, H**) of the beta variant. As a negative control, PBS was administered via intranasal route 2 h before infection (**A–H**). Body weight curve values represent means ± standard errors of the mean (n = 3 mice/group). Significant differences between the antibody treatment group and negative control are shown. ns, P > 0.05; \*, P < 0.05; \*\*, P < 0.0001, as determined by Student's t-test.

off their tails and dead at day 6), because the body weight of the mouse increased.

We then evaluated viral loads in the lungs of virus-challenged mice and pathogenic changes. The results showed that following 200 TCID<sub>50</sub> WIV04 challenge, the average viral RNA load in the lungs of mice in the PBS group was 10<sup>5</sup> copies/mL lung tissue, whereas viral RNA was negative in the antibody groups (P < 0.05; Fig. 3A–a). With 1000 TCID<sub>50</sub> challenge, the average viral RNA load in the PBS group reached 10<sup>8</sup> copies/mL, whereas that in the antibody groups remained low (P < 0.05; Fig. 3A–b). Similar results were observed for challenge with the beta variant (B.1.351); regardless of the dose, the average viral RNA load in the control groups was 10<sup>7</sup>–10<sup>8</sup> copies/mL in lung tissues, whereas that in the antibody groups was negative (Fig. 3A–c, F61) or low (10<sup>3</sup>–10<sup>4</sup> copies/mL; P < 0.05; Fig. 3A–c, -d). Similarly, histological analysis showed that almost all alveolar septa and cavities were normal when challenged with WIV04 wild strain or B.1.351 variant in the antibody groups (Fig. 3B–b, -e, -h, -c, -f, -i), and only mild lung damage was observed when challenged with 1000 TCID<sub>50</sub> B.1.351 variant (Fig. 3B–j, -k, -l). By contrast, mice in the PBS control group showed severe damage in the lung, characterized by diffuse

alveolar damage, including thickening of the alveolar septa, and extensive immune infiltration in the alveoli (Fig. 3B–a, -d, -g, -j).

### 3.3. Low-dose F61 and F61/H121 antibodies conferred *in vivo* protection against delta variant

We next determined whether F61 alone or the F61/H121 combination could confer *in vivo* protection against the delta variant of SARS-CoV-2. In challenge with 200 TCID<sub>50</sub> delta variant, high (10 and 20 mg/kg body weight) and low doses (5 mg/kg body weight) of F61 or F61/H121 neutralizing monoclonal antibodies provided complete protection against death and blocked body weight loss (P < 0.05; Fig. 4A and B, left and middle). Administration of 1.25 mg/kg F61 or F61/H121 also significantly protected mice from body weight loss and death, except one mouse (Fig. 4A and B middle). Furthermore, viral RNA copies in the control group reached 10<sup>9</sup> copies/mL in lung tissues, whereas those in the antibody groups, including the minimum dose antibody group, were significantly reduced or undetectable (under the limitation of detection, 10<sup>2.7</sup> copies/mL) (Fig. 4A and B right).

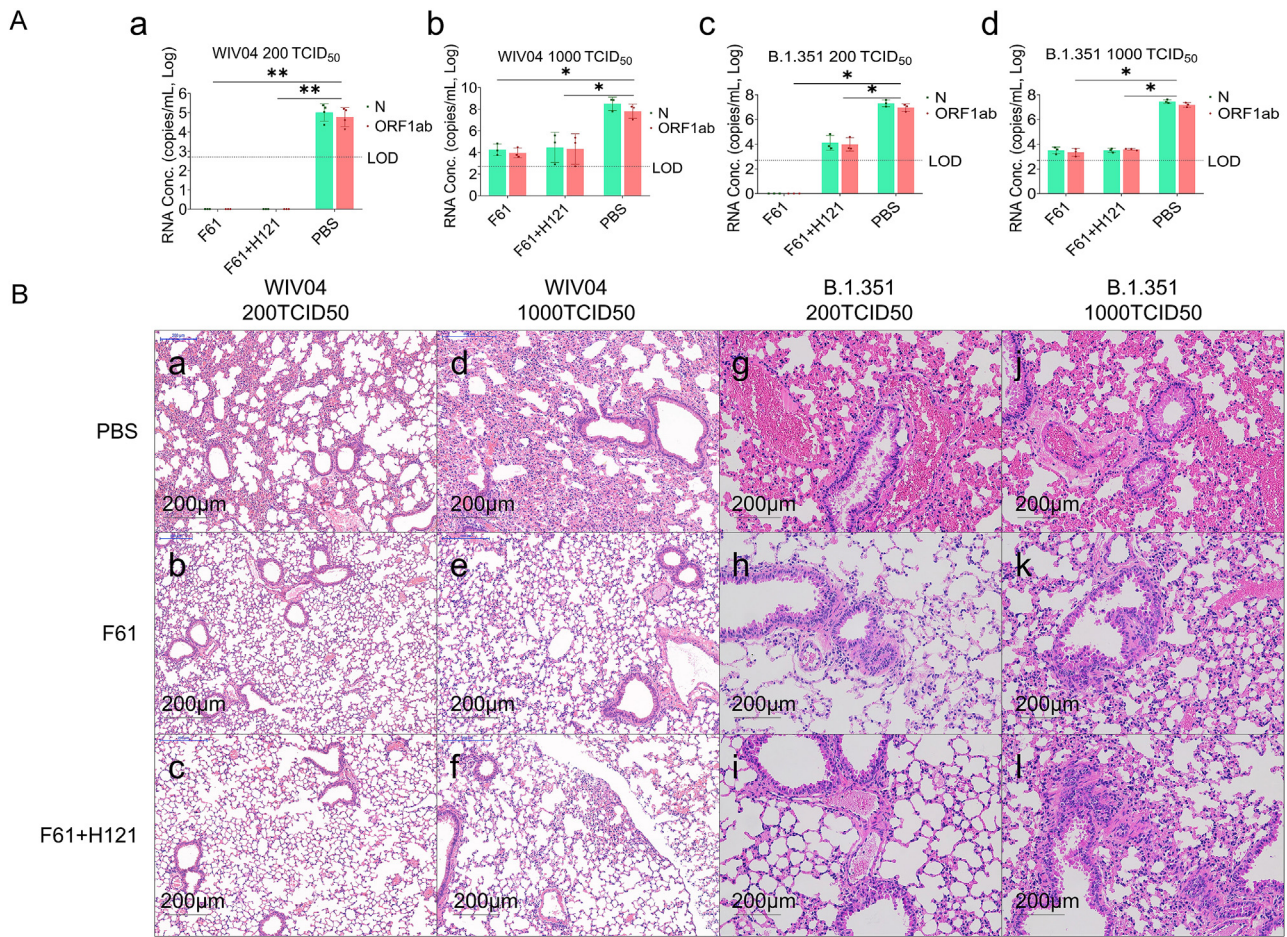


**Fig. 3.** Antibodies provided prophylactic protection against alterations in lung pathology following inoculation with the wild strain and B.1.351 variant of SARS-CoV-2. Mice were pretreated with 20 mg/kg F61 or F61+H121 cocktail via intranasal route 2 h before challenge with WIV04 or the beta variant. The same volume of PBS was administered via intranasal route in the negative control. Lungs were harvested from each group (n = 3). **A** Viral RNA levels in the lungs were measured by qRT-PCR (copies/mL). (**A-a**) 200 TCID<sub>50</sub> WIV04, (**A-b**) 1000 TCID<sub>50</sub> WIV04, (**A-c**) 200 TCID<sub>50</sub> beta variant, and (**A-d**) 1000 TCID<sub>50</sub> beta variant. **B** Histopathological analyses of mice pretreated with or without monoclonal antibodies and infected with SARS-CoV-2 strains. Lungs were fixed for sectioning before staining with hematoxylin and eosin. (**B-a–B-l**) Lung sections from mice treated PBS, F61, and F61/H121 cocktail before challenge with 200 TCID<sub>50</sub> WIV04 (**B-a–B-c**), 1000 TCID<sub>50</sub> WIV04 (**B-d–B-f**), 200 TCID<sub>50</sub> beta variant (**B-g–B-i**), or 1000 TCID<sub>50</sub> beta variant (**B-j–B-l**). All data points are shown, along with medians. ns,  $P > 0.05$ ; \*,  $P < 0.05$ ; \*\*,  $P < 0.0001$ , as determined by Student's *t*-test. Limit of detection (LOD), 500 copies/mL. Scale bars, 200  $\mu$ m.

In challenge with 1000 TCID<sub>50</sub> delta variant (later to be known equivalent to 1000 lethal dose 50% [LD<sub>50</sub>], data not shown), the high-dose antibody groups (20 mg/kg) were fully protected from the death and showed absence or a significant reduction of viral RNA in the lungs; the low-dose (5 mg/kg) were also protected with the survival rate of 83% (5/6) (Fig. 4D and E, left); only the minimum group (1.25 mg/kg) loss the body weight and the mice survival rate reduced to 33% (2/6) for F61 group and 50% (3/6) for F61+H121 group (Fig. 4D and E, middle and left).

However, we found that the lung viral RNA copies of PBS control groups in the protection efficacy assay of low dose antibody groups (5 or 1.25 mg/kg) were abnormally lower than that tested in all other PBS groups with delta variant challenge (supposed to be 10<sup>8–9</sup> copies/mL lung homogenates), and there was no significant differences between antibody and control groups (Fig. 4D and E, right). Later, we found the viral RNA copies in the brain tissue homogenates of these mice (reach to 10<sup>9.8</sup> copies/mL) were extremely higher than the copies in the lung tissue homogenates compared with the PBS group, the viral RNA copies in brains of both F61 and F61/H121 antibody groups were reduced (data not shown).

Histological analysis showed that almost all alveolar septa and cavities were normal in the antibody administration groups following challenge with 200 or 1000 TCID<sub>50</sub> delta variant, and only mild lung

damage was observed in the group administered 1.25 mg/kg monoclonal antibody. By contrast, mice in PBS control group showed severe lung damage, characterized by diffuse alveolar damage, including thickening of the alveolar septa, and extensive immune infiltration in the alveoli (data not shown).

#### 3.4. The protective effects F61 and F61/H121 antibodies against omicron variant

In November 2021, a new variant of SARS-CoV-2, the omicron (B.1.1.529), was reported from South Africa. This variant spreads rapidly, becoming the current major epidemic variant. Therefore, we next performed similar experiments using the omicron variant. Importantly, regardless of the dose or monoclonal antibody type, antibody treatment conferred protection against lethal challenge in K18-hACE2 mice inoculated with 200 TCID<sub>50</sub> omicron variant (Fig. 5A left), and body weights of mice remained normal throughout the experiments (Fig. 5A middle). Moreover, viral RNA in the lungs of mice was not detectable when the F61/H121 combination was used (Fig. 5A right). However, in the high-dose omicron challenge (1000 TCID<sub>50</sub> or 200 LD<sub>50</sub>), although high-dose antibody administration (20 mg/kg) protected mice from death and body weight loss, low-dose administration (5 mg/kg) only partially protected mice (Fig. 5B left and middle), and viral RNA was

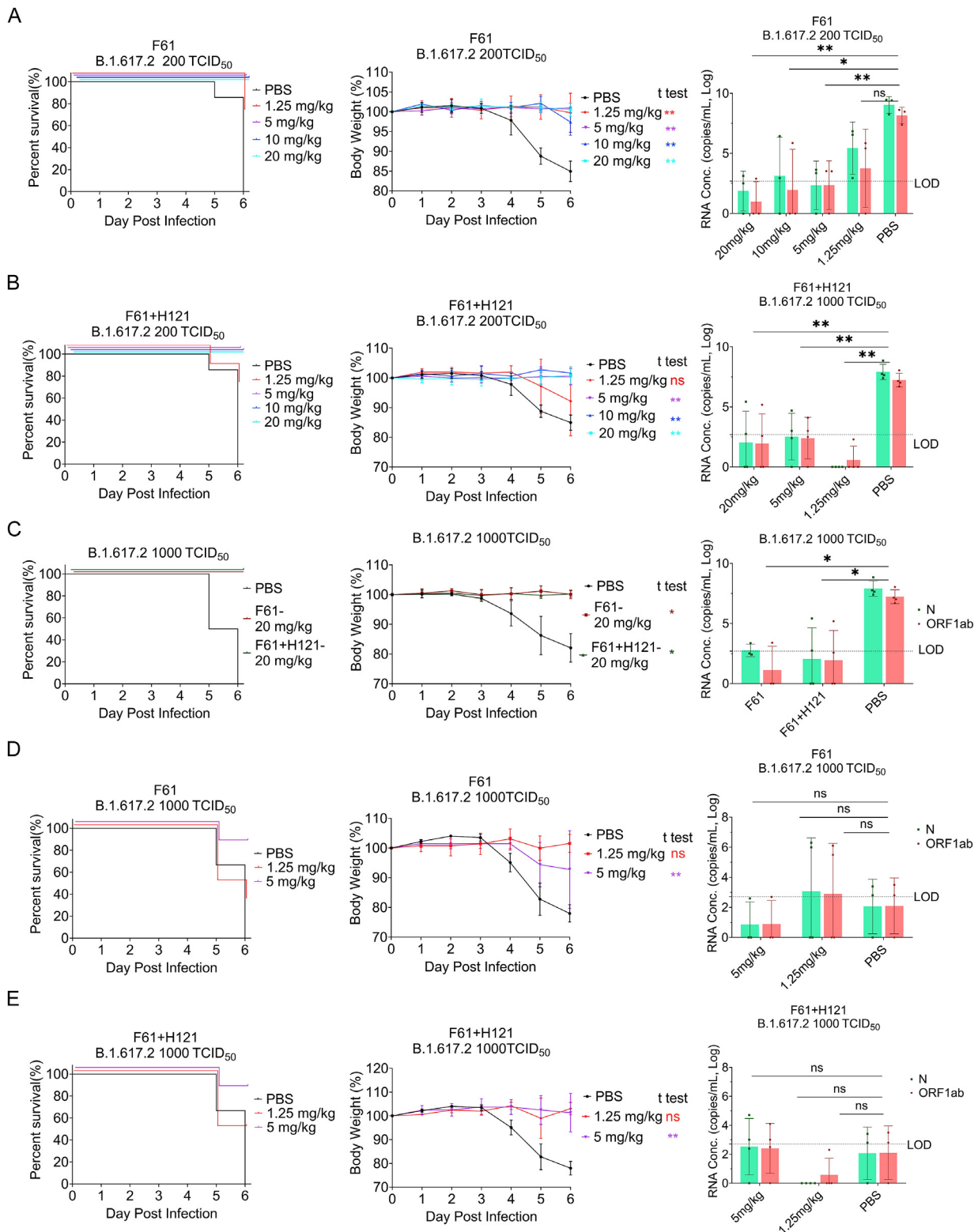


**Fig. 4.** Prophylactic effects of F61 or F61/H121 cocktail against delta SARS-CoV-2 (B.1.617.2) in K18-hACE2 mice. **A–B** Body weights, survival curves, and viral RNA loads in the lungs of K18-hACE2 mice treated with different doses of antibodies (1.25, 5, 10, and 20 mg/kg) F61 (**A**) or F61+H121 (**B**) cocktail via the intranasal route before infection with 200 TCID<sub>50</sub> delta variant. **C** Body weights, survival curves, and viral RNA loads in the lungs of K18-hACE2 mice treated with 20 mg/kg F61 or F61+H121 cocktail via intranasal route before infection with 1000 TCID<sub>50</sub> delta variant. **D–E** Body weights, survival curves and lung virus RNA detected by qRT-PCR of K18-hACE2 mice treated with a low dose antibodies (5 mg/kg or 1.25 mg/kg; **D** for F61, **E** for F61+H121 cocktail) via intranasal route before infection with 1000 TCID<sub>50</sub> of delta variants. Viral RNA loads were determined using qRT-PCR. Body weight curve values represent means ± standard errors of the means (n = 3–6 mice/group). Significant differences between the antibody treatment group and negative control are shown. All data points of virus load in the lungs are shown, along with the medians. ns, P > 0.05; \*, P < 0.05; \*\*, P < 0.0001, as determined by Student's *t* test. Limit of detection (LOD), 500 copies/mL.

detected in all dead or surviving mice. Despite this, the F61/H121 combination treatment significantly reduced viral RNA loads ( $10^3$ – $10^4$  copies/mL) in the lungs of mice compared with that in the PBS groups ( $10^7$  copies/mL, Fig. 5B, right).

4. Discussion

In this study, we systematically estimated the *in vivo* preventive and protective effects of F61 and H121 against SARS-CoV-2 variants, including beta (B.1.351), delta (B.1.617.2), and omicron (B.1.1.529). The bioavailability and distribution assays showed that the antibodies could be detected in the lungs of mice within 2 h after intranasal delivery and persisted in the lungs for at least 96 h. Intranasal administration of antibodies had obvious effects *in vivo*. Fully prophylactic protection was observed in all challenge groups when the antibodies were administered at a high dose (20 mg/kg), and significant prophylactic protection was also observed in the low-dose group (5 mg/kg). Additionally, F61/H121 administration also showed protection against the omicron variant when applied at a high dose. Thus, the broadly neutralizing monoclonal antibodies used in our study (F61 and H121) could be applied as potential prophylactic and therapeutic agents against current and emerging SARS-CoV-2 variants.

Our reliable findings showed that F61 and H121 had good protective effects, and strong correlations were observed among the evaluated parameters (i.e., body weight loss, survival rate, and viral load). In the control group, mice showed typical symptoms of disease, including body weight loss and high viral loads in the lungs. Here, except the most important biosafety issues, the personal operation and the K18-hACE2 mice (Hassan et al., 2020; Sun et al., 2020) were key factors to guarantee the authenticity of the animal experiments results and reliability of antibody evaluation results. In our study, totally we used 138 mice K18-hACE2 (6 batches of mice), only two mice died abnormally with no weight loss as we described in the result (Fig. 2C, F61 20 mg/kg group with 1000 TCID<sub>50</sub> WIV04 challenge). As we showed in the result (Fig. 4D and E), the tested K18-hACE2 mice in the low antibody dose groups with

1000 TCID<sub>50</sub> delta variant challenge have low RNA copies in lungs but high copies in brains. That might because of the abnormal high expression of ACE2 in brain. Even so, F61 or F61/H121 cocktail protected most of tested mice (5/6) from the high dose death challenge at a low dose (5 mg/kg body weight), and partial protection at the minimum antibody administration groups.

For the challenge of recent emerged omicron variant, the antibodies also showed effective protection, in particular use the F61/H121 cocktail bivalent antibodies. As we described previously (Qu et al., 2021), F61 recognizes a competitive epitope in ACE2-RBD binding domain, which may classified into class 1 neutralizing antigenic site (Barnes et al., 2020). H121 binds to an ACE2 non-competitive epitope located in a conserved side of RBD, which is closed to the class 4 antigenic site (Barnes et al., 2020). F61 directly blocks the virus binding with ACE2, while H121 may use mechanisms other than directly interfering with ACE2 binding. The cocktail of these two high affinity neutralizing antibodies could exhibit pan-sarbecovirus neutralization capacity to against most of SARS-CoV2 variants including omicron variants.

Furthermore, human immunoglobulin G antibodies were used instead of mouse antibodies in this study, which may have interfered with antibody function owing to interspecies difference (Yamin et al., 2021). Therefore, antibody evaluation in nonhuman primate animal models is essential for subsequent studies. In general, our current results suggested that F61 and H121 may have good preventive and protective effects against SARS-CoV-2 variants *in vivo*.

Currently, vaccines appear to be the solution for stopping the spread of SARS-CoV-2. However, the continuous emergence of new variants, particularly the substantially mutated variant omicron, may lead to reductions in the neutralizing activity of vaccine immune serum (Cao et al., 2021). Vaccine-induced antibodies may persist for a much shorter time than that required for new vaccine development (Kissler et al., 2020). Moreover, it is unrealistic to continuously develop novel vaccines targeting different SARS-CoV-2 variants. Compared with vaccines, antibodies are associated with rapid onset of immune responses, making them suitable prophylactic and therapeutic agents for application in

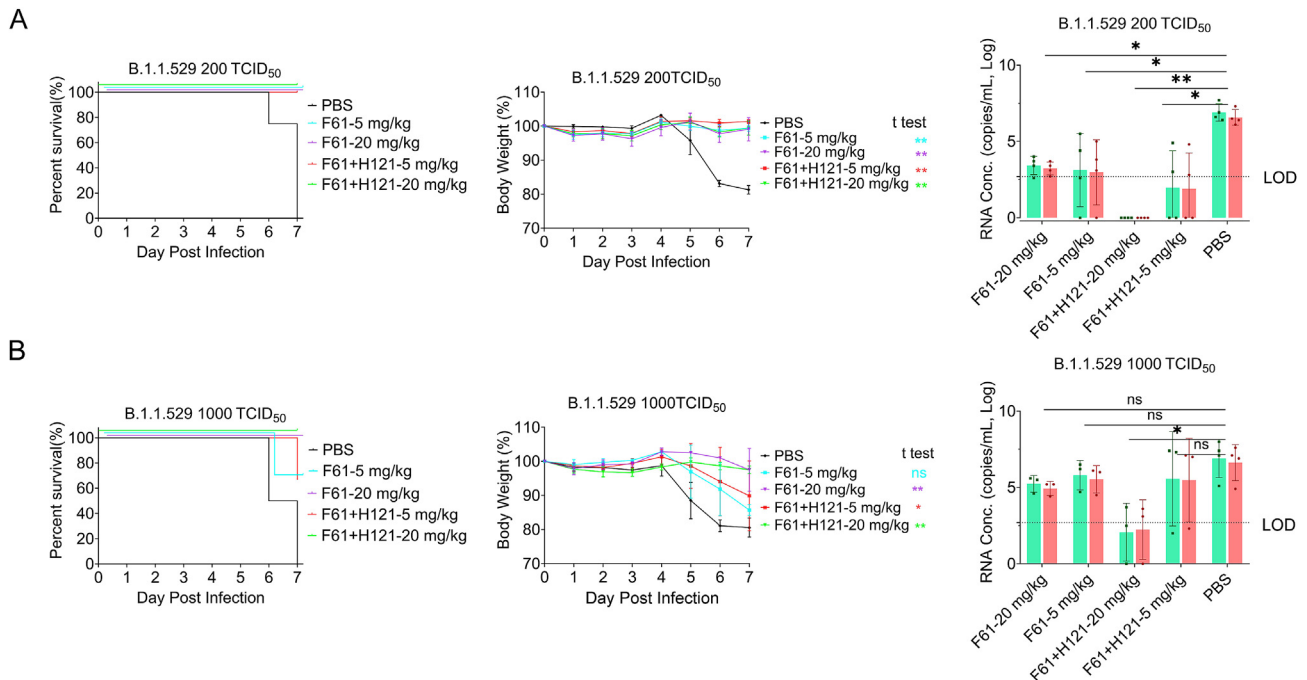


Fig. 5. Prophylactic effects of F61 or F61/H121 antibodies against the omicron SARS-CoV-2 (B.1.1.529) variant in K18-hACE2 mice. Body weights, survival curves, and viral RNA loads in the lungs of K18-hACE2 mice treated with difference doses of antibodies (5, 20 mg/kg) F61 or F61+H121 via intranasal route before infection with 200 TCID<sub>50</sub> (A) or 1000 TCID<sub>50</sub> (B) omicron variant. As a negative control, PBS was administered (A, B). Body weight curve values represent means ± standard errors of the means (n = 3–4 mice/group). Significant differences between the antibody treatment group and negative control are shown. All data points for viral load in the lungs are shown, along with the medians. ns,  $P > 0.05$ ; \*,  $P < 0.05$ ; \*\*,  $P < 0.0001$ , as determined by Student's *t*-test. Limit of detection (LOD), 500 copies/mL.



crowded settings, such as airports and large meetings. Furthermore, antibodies may play active roles in protection of populations at risk of virus exposure, such as medical staff, and in high-risk populations, such as the elderly and people with underlying conditions (Drożdżal et al., 2021). In total, seven monoclonal antibodies and combinations thereof have been approved or authorized for emergency use worldwide, most of which are administered intravenously for COVID-19 treatment and postexposure prevention (Drożdżal et al., 2021; WHO, 2021). Ronapreve and Evusheld, produced by AstraZeneca, can be used for pre-exposure prevention when administered subcutaneously (FDA EUA, 2022). After intravenous infusion, circulating monoclonal antibodies do not effectively target lung epithelial cells or the respiratory mucosa (DeFrancesco, 2020). Additionally, the concentrations of therapeutic antibodies in the lungs are thought to be 200–500 times lower than in the serum, although the concentrations that can be achieved in the upper respiratory tract are currently unknown (Iwasaki, 2016). Therefore, even for monoclonal antibodies with strong neutralizing efficacy *in vitro*, high-dose administration (e.g., grams) may be required for intravenous infusion to ensure sufficient antiviral effects in the lungs (Kreuzberger et al., 2021; Self et al., 2021). This would undoubtedly increase the cost of COVID-19 antibodies and limit their clinical applicability. As a prophylactic drug, nasal spray preparations of monoclonal antibodies may overcome these problems (FDA NEWS RELEASE, 2022; Tiwari et al., 2012). Intranasal administration directly establishes a defensive line in the respiratory tract and lungs to block the invasion of the virus (Leyva-Grado et al., 2015; Ku et al., 2021; Kwon, 2021). Because of these direct local effects, the dose of the drug can be greatly reduced, and safety is increased. In addition, as a noninvasive route, patients are more likely to show good compliance, and the treatment may be more suitable for use in families, potentially alleviating problems with the current shortage of medical resources. However, intranasal injection and conventional intravenous infusion of monoclonal antibodies can lead to different pharmacokinetic characteristics *in vivo* (DeFrancesco, 2020). Moreover, spray preparations and injection preparations have different requirements for drug characteristics (e.g., viscosity, stability, etc.), and the drug formulation may need to be altered for storage and daily use.

In this study, we found that the broadly neutralizing antibodies F61 and H121 could be detected in the lungs shortly after intranasal administration and persisted in the lungs for a long time. Furthermore, we showed that the two antibodies could be used as prophylactic drugs to prevent the transmission of SARS-CoV-2. Thus, we speculated that our antibodies may also show good *in vivo* therapeutic effects. In summary, the two antibodies evaluated in this study may be candidate therapeutic and preventive drugs with a wide range of applications. Further studies are needed.

#### Data availability

All the data generated during the current study are included in the manuscript.

#### Ethics statement

This study was approved by the Institutional Animal Ethical Committee of Wuhan Institute of Virology, Chinese Academy of Sciences (approval no. WIVA32202104) and the Experimental Animal Welfare and Ethical Review Board of Wuhan Institute of Biological Products Co. Ltd (protocol WIBP-AII442021005). The experiments conducted in strict accordance with the recommendations in the Guide for the Care and Use of Laboratory Animals established by the People's Republic of China.

#### Author contributions

Jia Lu, Rongjuan Pei, Qiu Zhang, Ding Gao, Cuiqin Liang: conceptualization, data curation, investigation, methodology; Qiangling Yin, YuanYuan Qu and Lina Sun: formal analysis, validation, visualization,

writing – original draft; Yongbing Pan, Wei Wu, Jiandong Li, Zejun Wang, Zongqiang Cui, Jingwen Yang: resources, software, software; Xinguo Li, Dexin Li, Shiwen Wang, Kai Duan: project administration, supervision. Xiaoming Yang, Mifang Liang, and Wuxiang Guan: funding acquisition, writing – review & editing. All authors read and approved the final manuscript.

#### Conflict of interest

The authors declare that they have no conflict of interest.

#### Acknowledgments

We thanks Biosafety experts Dr. Donglin Song from Wuhan Institute of Virology, Chinese Academy of Sciences, Dr. Qiang Wei from Institute of Laboratory Animal Science, CAMS&PUMC for the biosafety assistance in all mice experiments related to the wild or variants of SARS-CoV-2 virus challenges in ABSL-3 laboratory. This work was supported by National Key Research and Development Program of China (2021YFC2600200, 2017YFA0205100).

#### References

- Andreano, E., Piccini, G., Licastro, D., Casalino, L., Rappuoli, R., 2021. SARS-CoV-2 escape *in vitro* from a highly neutralizing COVID-19 convalescent plasma. *Proc. Natl. Acad. Sci. U. S. A.* 118, e2103154118.
- Barnes, C.O., Jette, C.A., Abernathy, M.E., Dam, K.A., Esswein, S.R., Gristick, H.B., Maluyutin, A.G., Sharaf, N.G., Huey-Tubman, K.E., Lee, Y.E., Robbiani, D.F., Nussenzweig, M.C., West Jr., A.P., Bjorkman, P.J., 2020. SARS-CoV-2 neutralizing antibody structures inform therapeutic strategies. *Nature* 588, 682–687.
- Callaway, E., 2021. Heavily mutated Omicron variant puts scientists on alert. *Nature* 600, 21.
- Cao, Y., Wang, J., Jian, F., Xiao, T., Song, W., Yisimayi, A., Huang, W., Li, Q., Wang, P., An, R., 2021. Omicron escapes the majority of existing SARS-CoV-2 neutralizing antibodies. *Nature* 602, 657–663.
- Chen, J., Wang, R., Gilby, N.B., Wei, G.W., 2021. Omicron Variant (B.1.1.529): infectivity, vaccine breakthrough, and antibody resistance. *J. Chem. Inf. Model.* 62, 412–422.
- DeFrancesco, L., 2020. COVID-19 antibodies on trial. *Nat. Biotechnol.* 38, 1242–1252.
- Drożdżal, S., Rosik, J., Lechowicz, K., Machaj, P., Szostak, B., Przybyciński, J., Lorzadeh, S., Kotfis, K., Ghavami, S., Łos, M.J., 2021. An Update on Drugs with Therapeutic Potential for SARS-CoV-2 (COVID-19) Treatment. *Drug Resist Updat.* p. 100794.
- Du, L., Zhao, G., He, Y., Guo, Y., Zheng, B.J., Jiang, S., Zhou, Y., 2007. Receptor-binding domain of SARS-CoV spike protein induces long-term protective immunity in an animal model. *Vaccine* 25, 2832–2838.
- Food and Drug Administration (FDA). Emergency use authorization. <https://www.fda.gov/emergency-preparedness-and-response/mcm-legal-regulatory-and-policy-framework/emergency-use-authorization>. (Accessed 22 January 2022).
- Food and Drug Administration (FDA) FDA NEWS RELEASE. Coronavirus (COVID-19) update: FDA authorizes new long-acting monoclonal antibodies for pre-exposure prevention of COVID-19 in certain individuals. <https://www.fda.gov/news-events/press-announcements/coronavirus-covid-19-update-fda-authorizes-new-long-acting-monoclonal-antibodies-pre-exposure>. (Accessed 22 January 2022).
- GISAID, 2022. SARS-CoV-2 (hCoV-19) mutation reports. <https://outbreak.info/>. (Accessed 22 January 2022), 2022.
- Hassan, A.O., Case, J.B., Winkler, E.S., Thackray, L.B., Kafai, N.M., Bailey, A.L., McCune, B.T., Fox, J.M., Chen, R.E., Alsoussi, W.B., 2020. A SARS-CoV-2 infection model in mice demonstrates protection by neutralizing antibodies. *Cell* 182, 744–753 e4.
- He, Y., Zhou, Y., Liu, S., Kou, Z., Li, W., Farzan, M., Jiang, S., 2004. Receptor-binding domain of SARS-CoV spike protein induces highly potent neutralizing antibodies: implication for developing subunit vaccine. *Biochem. Biophys. Res. Commun.* 324, 773–781.
- Hoffmann, M., Krüger, N., Schulz, S., Cossmann, A., Rocha, C., Kempf, A., Nehlmeier, I., Graichen, L., Moldenhauer, A.S., Winkler, M.S., 2021. The Omicron variant is highly resistant against antibody-mediated neutralization – implications for control of the COVID-19 pandemic. *Cell* 185, 447–456 e11.
- Iwasaki, A., 2016. Exploiting mucosal immunity for antiviral vaccines. *Annu. Rev. Immunol.* 34, 575–608.
- Jiang, S., Bottazzi, M., Du, L., Lustigman, S., Tseng, C., Curti, E., Jones, K., Zhan, B., Hotez, P.J., 2012. Roadmap to developing a recombinant coronavirus S protein receptor-binding domain vaccine for severe acute respiratory syndrome. *Expert Rev. Vaccines* 11, 1405–1413.
- Kissler, S.M., Tedijanto, C., Goldstein, E., Grad, Y.H., Lipsitch, M., 2020. Projecting the transmission dynamics of SARS-CoV-2 through the postpandemic period. *Science* 368, 860–868.
- Kreuzberger, N., Hirsch, C., Chai, K.L., Tomlinson, E., Khosravi, Z., Popp, M., Neidhardt, M., Piechotta, V., Salomon, S., Valk, S.J., 2021. SARS-CoV-2—neutralising

- monoclonal antibodies for treatment of COVID-19. *Cochrane Database Syst. Rev.* 9, CD013825.
- Ku, Z., Xie, X., Hinton, P.R., Liu, X., An, Z., 2021. Nasal delivery of an IgM offers broad protection from SARS-CoV-2 variants. *Nature* 595, 718–723.
- Kwon, D., 2021. Antibody-laden nasal spray could provide COVID protection and treatment. *Nature*. <https://doi.org/10.1038/d41586-021-01481-2>.
- Lei, C., Yang, J., Hu, J., Sun, X., 2021. On the calculation of TCID<sub>50</sub> for quantitation of virus infectivity. *Virolog. Sin.* 36, 141–144.
- Leyva-Grado, V.H., Tan, G.S., Leon, P.E., Yondola, M., Palese, P., 2015. Direct administration in the respiratory tract improves efficacy of broadly neutralizing anti-influenza virus monoclonal antibodies. *Antimicrob. Agents Chemother.* 59, 4162–4172.
- National Institutes of Health (NIH), 2021. COVID-19 treatment guidelines panel. Coronavirus disease 2019 (COVID-19) treatment guidelines. <https://www.Covid19treatmentguidelines.nih.gov/>. (Accessed 22 January 2022).
- Piccoli, L., Park, Y.J., Tortorici, M.A., Czudnochowski, N., Velesler, D., 2020. Mapping neutralizing and immunodominant sites on the SARS-CoV-2 spike receptor-binding domain by structure-guided high-resolution serology. *Cell* 183, 1024–1042 e21.
- Planas, D., Saunders, N., Maes, P., Guivel-Benhassine, F., Planchais, C., Buchrieser, J., Bolland, W.H., Porrot, F., Staropoli, I., Lemoine, F., 2021. Considerable escape of SARS-CoV-2 Omicron to antibody neutralization. *Nature* 602, 671–675.
- Qu, Y., Zhang, X., Wang, M., Sun, L., Jiang, Y., Li, C., Wu, W., Chen, Z., Yin, Q., Jiang, X., 2021. Antibody cocktail exhibits broad neutralization against SARS-CoV-2 and SARS-CoV-2 variants. *Virolog. Sin.* 36, 934–947.
- Self, W.H., Sandkovsky, U., Reilly, C.S., Vock, D.M., Gottlieb, R.L., Mack, M., Golden, K., Dishner, E., Vekstein, A., Ko, E.R., 2021. Efficacy and safety of two neutralising monoclonal antibody therapies, sotrovimab and BRII-196 plus BRII-198, for adults hospitalised with COVID-19 (TICO): a randomised controlled trial. *Lancet Infect. Dis.* S1473–3099 (21), 751–759.
- Starr, T.N., Greaney, A.J., Addetia, A., Hannon, W.W., Bloom, J.D., 2021. Prospective mapping of viral mutations that escape antibodies used to treat COVID-19. *Science* 371, 850–854.
- Sun, S.H., Chen, Q., Gu, H.J., Yang, G., Wang, Y.X., Huang, X.Y., Liu, S.S., Zhang, N.N., Li, X.F., Xiong, R., 2020. A mouse model of SARS-CoV-2 infection and pathogenesis. *Cell Host Microbe* 28, 124–133 e4.
- Tiwari, G., Tiwari, R., Bannerjee, S., Bhati, L., Pandey, S., Pandey, P., Sriwastawa, B., 2012. Drug delivery systems: an updated review. *Int. J. Pharm. Investig.* 2, 2–11.
- Viana, R., Moyo, S., Amoako, D.G., Tegally, H., Scheepers, C., Althaus, C.L., Anyaneji, U.J., Bester, P.A., Boni, M.F., Chand, M., 2022. Rapid epidemic expansion of the SARS-CoV-2 Omicron variant in southern Africa. *Nature*. <https://doi.org/10.1038/s41586-022-04411-y>.
- Wang, N., Shang, J., Jiang, S., Du, L., 2020. Subunit vaccines against emerging pathogenic human coronaviruses. *Front. Microbiol.* 11, 298.
- Weisblum, Y., Schmidt, F., Zhang, F., Dasilva, J., Bieniasz, P.D., 2020. Escape from neutralizing antibodies by SARS-CoV-2 spike protein variants. *Elife* 9, e61312.
- World Health Organization (WHO), 2022. Tracking SARS-CoV-2 variants. <https://www.who.int/en/activities/tracking-SARS-CoV-2-variants/>. (Accessed 22 January 2022).
- World Health Organization (WHO), 2021. WHO coronavirus disease (COVID-19) dashboard. <https://covid19.who.int/>. (Accessed 13 February 2022).
- Yamin, R., Jones, A.T., Hoffmann, H.H., Schäfer, A., Kao, K.S., Francis, R.L., Sheahan, T.P., Baric, R.S., Rice, C.M., Ravetch, J.V., 2021. Fc-engineered antibody therapeutics with improved anti-SARS-CoV-2 efficacy. *Nature* 599, 465–470.